ELSEVIER

Journal of University of Science and Technology Beijing
Volume 15, Number 2, April 2008, Page 125

Materials

Microstructure and mechanical properties of railway wheels manufactured with low-medium carbon Si-Mn-Mo-V steel

Mingru Zhang[1,2] *and Haicheng Gu*[1]

1) State Key Laboratory for Mechanical Behavior of Materials, Xi'an Jiaotong University, Xi'an 710049, China
2) Technical Center, Maanshan Iron & Steel Co. Ltd., Maanshan 243000, China
(Received 2007-05-28)

Abstract: The suitability of carbide-free bainite steel as railway wheel materials was investigated. The low-medium carbon Si-Mn-Mo-V steel was designed to make railway wheels by forging and rolling. The slack quenching with water was conducted on the tread of rim section by programmed control to simulate isothermal heat treatment after being austenitized. Microstructures and mechanical properties have been studied. The results indicate that the microstructure of the rim is mainly carbide-free bainite, and the mixed microstructure of bainitic ferrite and granular bainite is observed in web and hub. The mechanical properties are superior to both the standard requirements and the commercial production, such as CL60 plain carbon. The Charpy impact energy is relatively high at room and/or subzero temperatures. The force-displacement curves and fractographies reveal the excellent ability of resistance to crack initiation and propagation.

Key words: wheel steel; carbide-free bainite; microstructure; mechanical properties

[*This work was financially supported by the Ministry of Railway of China and the National High-Tech Research and Development Program of China (863 Program, No. 2003AA331160).*]

1. Introduction

Chinese railway will continue to develop high-speed passenger trains, heavy haul freight transportation and various kinds of special wagons. It requires higher safety and reliability, as well as requirements for wheel material quality, assembly process, static balance and test standards [1-2]. Railway wheels are the key parts that must be superior to wear resistance, thermal crack, fatigue and fracture leading to a sudden catastrophic failure. In the present time, the wheels are made of medium-high carbon grade steels with the carbon content of 0.45wt%-0.75wt%. The microstructures are pearlite-ferrite. The phase interfaces between ferrite and cementite in pearlite are crack initiation sources. Previous improvements in wheel steels include the enhancements of the existing eutectoid carbon pearlite-ferrite wheel steels by micro-alloying and cleaner steels made possible by the improved steel-making process. However, these conventional classes of steels have a limited scope for further significant improvement because of the relatively low toughness, ductility, and fatigue resistance [3-5].

During a wheel-rail slide or tread braking, the temperature is high enough to austenitize the tread close to the contact surface. After that, the tread is rapidly cooled by heat conduction into the rest of the wheel when the wheel set starts rolling again and thus martensite is formed in the surface layer. The carbon content or the starting temperature M_s for martensite phase change affects the transformation of martensite. Cracks can initiate on the tread by rapid heating and cooling when the wheel slides on the rail during intended or unintended braking events. The initiation and propagation of cracks lead to spalling after the thermal damage repeats several times. High carbon content facilitates the formation and propagation of thermal cracks [6].

Hardness and strength are considered the primary

Corresponding author: Mingru Zhang, **E-mail:** zhangmingru@mgjszx.com
Also available online at www.sciencedirect.com

indicators of wheel service performance. Wear resistance has often been associated with increased hardness to obtain a deep usable tread with uniform hardness; however, yield strength has a major influence on the resistance to rolling contact fatigue (RCF) as it will dictate the cyclic strain amplitude caused by rolling contact stresses. The normal contact and shear stresses applied through rolling can cause cracks on the surface of wheels and/or rails [7-8].

The wheels of pearlite-ferrite steels fail to resolve these two problems at the same time because of low yield strength and high carbon content, and it is more difficult to prevent spalling or shelling under the condition of heavy load and high speed.

For the long research process of the bainitic theory and application, scientists and technicians have realized that high silicon (~2wt%) hinders the precipitation of brittle carbide during phase transformation [9-14]. If the steel has good hardenability and the cooling rate after austenitizing is high, the microstructure is carbide-free bainite without carbides, that is, the thin film of retained austenite enriched with high carbon content distributes between the laths of bainitic ferrites. Because of supersaturation strengthening and fine laths and/or subunits strengthening, the yield strength of carbide-free bainite is higher than that of pearlite-ferrite under similar tensile strength level. This investigation studies the possibility of carbide-free bainite steel used for the manufacture of railway wheels. Newly experimental Si-Mn-Mo-V steel was designed. The wagon wheels of 840 mm in diameter were made. The microstructures and mechanical properties were evaluated and compared with those for CL60 wheels of conventional carbon grade.

2. Experimental procedure

The experimental low-medium carbon Si-Mn-Mo-V steel was designed and optimized on the basis of laboratory researches and small-scale trial. The heat of trial steel was melted in a 40 t electric arc furnace, secondary steel-making processes were performed in a ladle furnace (LF) and a vacuum-degassing (VD) vessel to maintain the [H] content at 1.70 ppm, and then was poured into round ingots with a diameter of 420 mm and a weight of 2.93 t at Maanshan Iron & Steel Co. Ltd. After stress relief annealing and cutting, the round ingots were forged and rolled into the wheels of 840 mm in diameter for wagon transportation. During heat treatment, the wheels were heated to 910°C after soaking for 2 h, and slack quenching with water were conducted on the tread of rim section by programmed control to simulate the isothermal heat treatment. Two wheels were press-fitted with an axle into the bore of hub for assembly test. Two wheels were studied and analyzed according to Chinese railway standard TB/T2708-1996. Eight wheels were run on a special experimental route over 180000 km with a periodic monitor. And others underwent a series of experiments to optimize the fabrication technology.

The chemical composition was measured using an ARL 4460 optical emission spectrometer. The metallographic specimens with a size of 25 mm×25 mm×25 mm were taken from the rim, web and hub section, respectively, and were for inclusion and microstructure analysis. Simultaneously, the microstructures were observed and analyzed using a transmission electron microscope (TEM). The content of retained austenite was determined by an X-ray diffractometer with the diffraction peak integral intensity of {220}, {311} crystal plane [15-16].

The Brinell hardness numbers (HB) were measured on the full section with Digital Brinell Testor 970/3000. The tensile specimens of the rim, taken from 30 mm under the tread, were ϕ15 mm×60 mm short proportion specimens, and the web or hub tensile specimens were ϕ10 mm×50 mm proportion specimens using the WAW-Y500A material testing system. Impact specimens were taken from the rim, web, and hub respectively, and the standard 10 mm×10 mm×55 mm Charpy U2-notch specimens were used. The Charpy test was conducted at room temperature and subzero temperatures using an Amsler/Roell RKP450 instrumented impact testing machine. All fractographies of the specimens were inspected and analyzed using a Philips XL30 scanning electron microscope (SEM) equipped with an energy dispersive spectrometer.

To compare with the pearlite-ferrite wheel, the CL60 wheel of industrial scale production was also tested.

3. Experimental results

3.1. Chemical composition and microstructures

The chemical compositions of bainitic and pearlite-ferrite wheel steels are shown in Table 1. The carbide-free bainite steel is low-medium carbon Si-Mn-Mo-V steel with sufficient silicon to prevent the precipitation of carbides during phase transformation at slow cooling rates, sufficient manganese for the purpose of increasing hardenability, and some other alloys, such as molybdenum and vanadium. The addition of molybdenum and vanadium facilitates to achieve the desired hardenability for obtaining uniform hardness and is beneficial for achieving finer

grain size and higher tensile strength and toughness. The addition of molybdenum also represses temper embrittlement.

Table 1. Chemical composition of bainitic and CL60 wheel steels **wt%**

Steel	C	Si	Mn	Mo	V	S	P	Cr	Ni	Cu	Fe
Bainitic	0.19	1.44	1.82	0.26	0.07	0.004	0.013	0.09	0.22	0.03	Bal.
CL60	0.60	0.26	0.74	—	—	0.003	0.010	≤0.25	≤0.25	≤0.25	Bal.

For the bainitic wheel, the rim microstructure at the range of 55 mm below the tread is mainly carbide-free bainite, and that of the web and hub is granular bainite and bainitic ferrite, respectively, as shown in Figs. 1(a)-(c). To distinguish the type of bainite and the morphology of retained austenite, TEM was used to go further into determining the microstructures. The morphology of retained austenite in the rim is the film among bainitic ferrite laths or sub-laths whose width is 10-30 nm, as shown in Figs. 2(a) and (b). The volume fraction of retained austenite is about 4vol%-9vol%, and martensite structure or carbide precipitation is not found by X-ray diffraction spectrum.

CL60 is a typically wheel steel with the carbon content of 0.60wt% and the microstructure is pearlite-ferrite. There are essential differences in carbon and alloying element contents and microstructures of these two kinds of wheel steels.

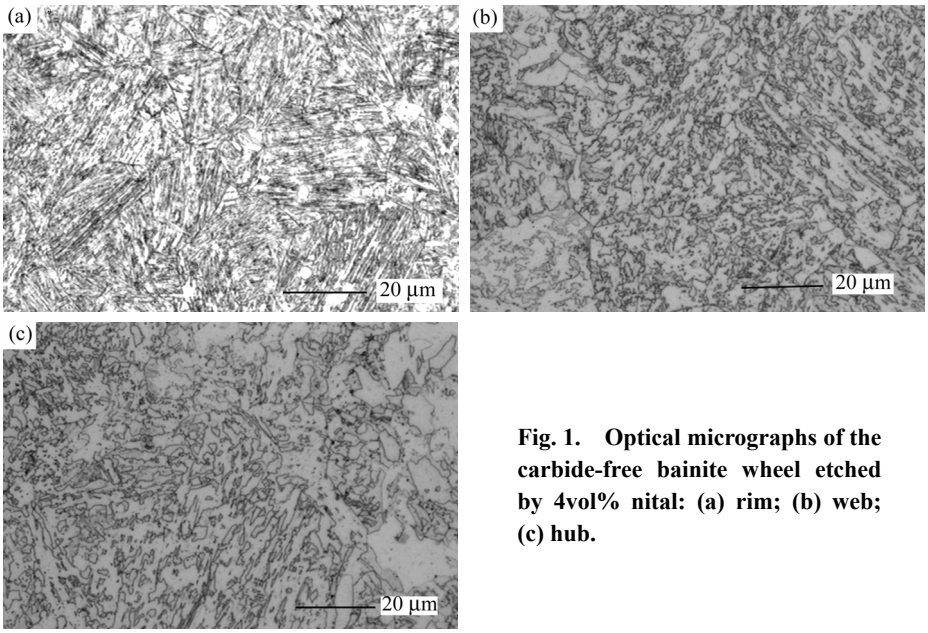

Fig. 1. Optical micrographs of the carbide-free bainite wheel etched by 4vol% nital: (a) rim; (b) web; (c) hub.

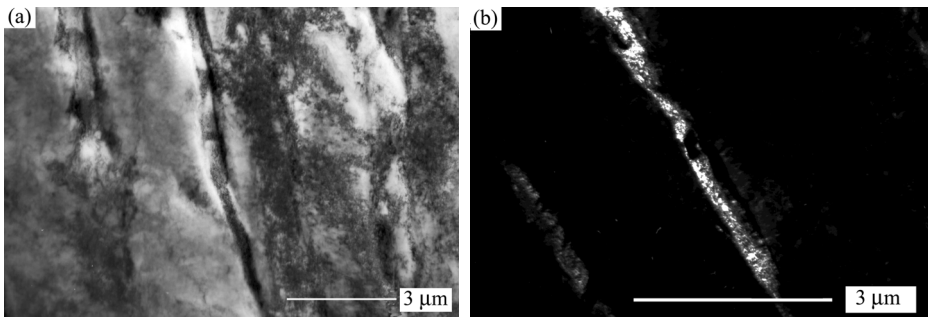

Fig. 2. TEM micrographs of the carbide-free bainite wheel rim: (a) bright-field image; (b) corresponding dark-field image.

3.2. Mechanical properties

The mechanical properties of yield strength (YS), ultimate tensile strength (UTS), elongation (EL), reduction of area (RA), hardness below the tread 30 mm, and Charpy impact energy E_t broken at room temperature with the U-2 notch, as well as the conventional wheel standard requirements, are shown in Table 2.

The hardness profiles at the cross surface of the bainitic wheel are shown in Fig. 3. The hardness of the bainitic wheel is relatively higher and more uniform throughout various locations within the all-section, and the hardness level exceeds HB 37 below the tread 30 mm than that of a conventional CL60 wheel (an

average hardness of HB 273 shown in Table 2). By comparing the hardness of the bainitic wheel, the hardness in the rim, web or hub, almost is at a similar level although the cooling rates are quite different, and it is reasonable to assume that the surface hardness is maintained throughout a typical rim cross-section. The cooling rate of the rim is the fastest because of tread slack quenching, and the cooling rate of the hub is the slowest. The microstructures demonstrate the difference of the cooling rates, as shown in Fig. 1. The bainitic wheel steel has higher hardenability compared with CL60 by metallographic structures and hardness profiles.

Table 2. Mechanical properties of bainitic and CL60 wheels

Materials	YS / MPa	UTS / MPa	EL / %	RA / %	Hardness (HB)	Impact energy / J
Bainitic wheel rim	860	1090	15	50	310	159
Bainitic wheel web	585	1020	13	37	295	91
Bainitic wheel hub	590	990	12	23	290	95
CL60 wheel rim	665	1020	15	34	273	34 (web)
Standard TB/T2708	—	≥910	≥10	≥14	265-320	≥16 (web)

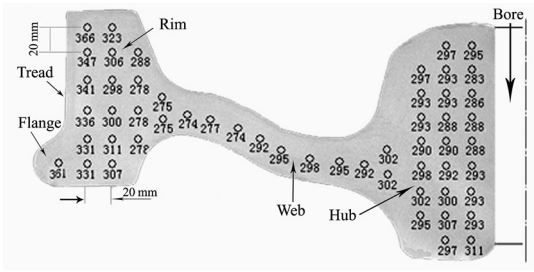

Fig. 3. Brinell hardness (HB) profiles of the wheel.

Fig. 4 shows the total impact energy E_t in the rim and web at different testing temperatures for the bainitic wheel. The force-displacement curves reveal the excellent ability of resistance to crack initiation and propagation, because the crack forming energy E_i and the crack propagation energy E_p both are higher than those of the CL60 wheel by the instrumented impact testing machine.

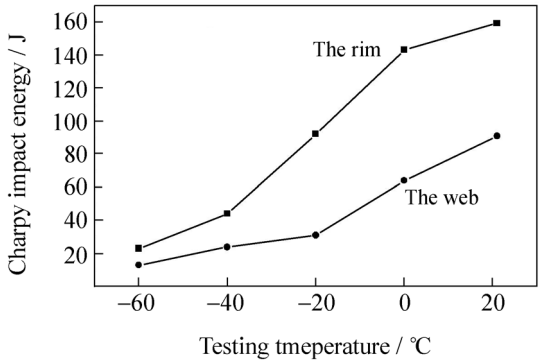

Fig. 4. Impact energy E_t at different testing temperatures.

3.3. Fractographies of tensile and impact fractures

After tensile and Charpy impact tests, the fractographies of specimens were inspected and analyzed using SEM. The fractograph of the tensile specimen about the stable propagation appearance is shown in Fig. 5. The fractographs of the rim impact specimens broken at room temperature are shown in Figs. 6(a)-(c), respectively.

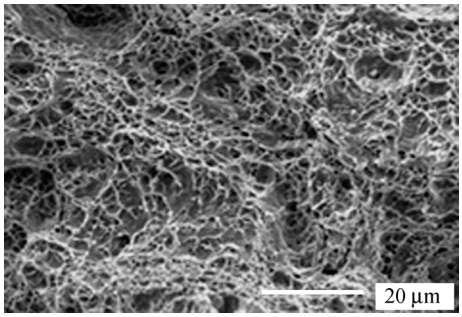

Fig. 5. Tensile fracture of the rim about stable propagation.

4. Discussion

4.1. Material design and thermal damage

Wheel materials are subjected to various stresses and transient thermal loads during running and through tread braking. Skids and burns in present pearlite-ferrite wheel steels invariably result in spalling as the regions with brittle high carbon martensite formed by rapid cooling fracture and separate from the tread surface. To improve thermal damage, as well as the ductility and toughness at an equal ultimate tensile strength, the principle of the latest design for wheel steels is to decrease carbon content. The essence of the problem is carbon content leading to inhomogeneity in sections of wheels, because the microstructure and properties of medium carbon steels are too sensitive to cooling rate. So low carbon content is selected, and more reasons for this decision will be elucidated later. The carbide-free bainite wheel steel is low-medium carbon alloying steel; the martensite phase transformation start point M_s of the steel is about 370°C. The martensite phase transformation start point M_s of retained austenite is very low, because the film retained austenite richens carbon [17-20]. When the wheel is heated to the austenitizing

temperature due to heating by braking and then rapidly cooled in a moment, the heating is so fast that the carbon in the original retained austenite has no time to diffuse. Low carbon austenite is formed in the process of heating, and is then transformed into carbon-free bainite or auto-temped martensite during natural cooling. The martensite phase transformation start point M_s of high carbon retained austenite is still low, and it is difficult to transform into martensite even at low temperature. The products of phase transformation still are carbide-free bainite. It is expected that the whole performance of wheels, including the resistance to shelling and thermal damage, will be improved with this low-medium carbon Si-Mn-Mo-V steel whose rim microstructure is carbide-free bainite.

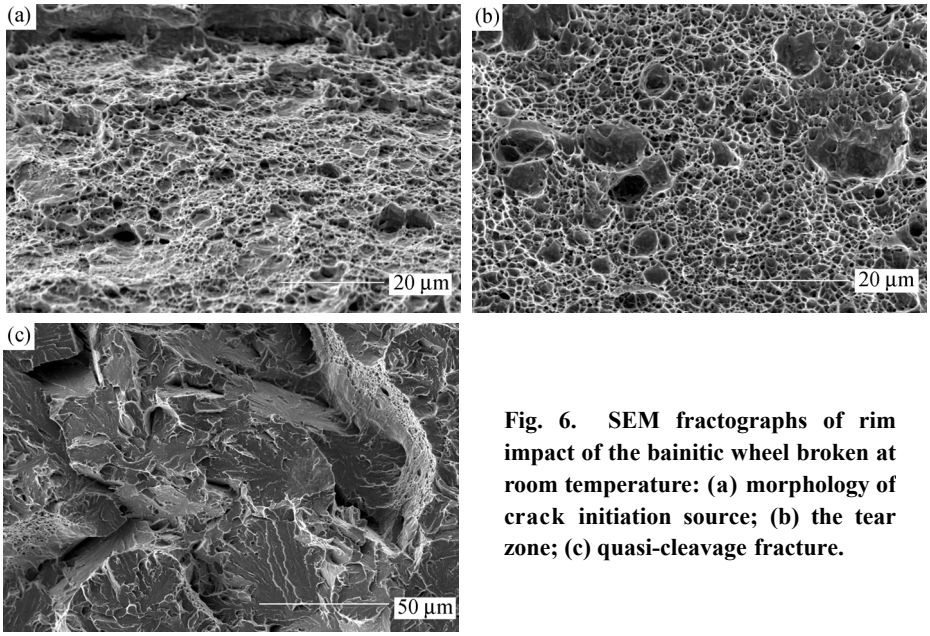

Fig. 6. SEM fractographs of rim impact of the bainitic wheel broken at room temperature: (a) morphology of crack initiation source; (b) the tear zone; (c) quasi-cleavage fracture.

Carbide-free bainite steel, applied on wheel manufacture, can be produced with cheap alloying additions, such as silicon and manganese. As long as the chemical composition is designed to assure the microstructure at the range to 55 mm below the tread is mainly carbide-free bainite, the wheel will satisfy the new development of railway transportation, and may provide the improved resistance to rolling contact fatigue, and the minimize sensitivity to thermal damage.

4.2. Hardness and strength

To improve wear and shelling, higher yield strength and hardness are necessary, as well as good plasticity and toughness simultaneously. Decreasing hardness with depth from the tread surface is typical for the conventional pearlite-ferrite wheel, as the cooling rates promoting pearlite refinement are not uniform throughout the rim cross-section due to large thermal mass of the wheel and the relative low hardenability of these steels. High carbon content generally contributes to a higher hardness and reduces the hardness gradient. Micro-alloying substantially increases hardness, while also slightly decreases the hardness gradient. The treads are in the elastic region under the major applied stresses, but triaxial stresses from the wheel-rail contact will inevitably exceed the elastic limit. Shear stresses caused by Hertz contact stresses are higher than the permitted shear stress of the steel, especially, having the maximum shear stresses under the tread 1-5 mm, and the Hertz contact fatigue is improved by increasing yield strength [9]. Compared with those of the pearlite-ferrite wheel, the values of yield strength, hardness and plasticity of the carbide-free bainite wheel are much higher, and the hardness gradient reduces.

According to Fig. 5, the microscopic appearance of the fracture surface also manifests an excellent combination of strength with toughness. The crack morphology of the fracture surface with the inner wall is shown and it indicates the ductile tearing appearance with a considerable amount of plastic deformation. There are numerous secondary cracks in the fracture surface. Secondary cracking also is one of the characterizations of fracture surface according with the propagation mechanism of the crack path. The secondary cracks of tensile fracture consume a great deal of energy, relax stress concentration, weaken the stress peak of crack tips and reduce the propagation speed of main cracks and/or change the crack propagation direction.

For the pearlite-ferrite wheel steel, the secondary cracks of tensile fracture are the patterns of quasi-cleavage.

4.3. Charpy impact Toughness

The Charpy impact value is one of the fundamental properties of material toughness. The carbide-free bainite steel wheel has extraordinary impact toughness at room and/or subzero temperatures. Fig. 6(a) shows the zone of crack initiation and is characterized by dimples, and there is an obvious stretched zone in the root of the specimen notch. The stretched zone is the pattern of ripple and has plastic deformation with shallow dimple morphologies and strain hardening. The width of the stretched zone is about 32 μm. Fig. 6(b) shows the zone of tearing with crack stable propagation and is characterized by dimples. Fig. 6(c) shows the zone of crack unstable propagation and is characterized by distinct quasi-cleavage. The SEM fractographies of impact broken at room and/or subzero temperatures reveal the excellent ability of resistance to crack initiation and propagation.

Furthermore, the ductility and toughness at an equal ultimate strength are beneficial to the reliability and safety of wheels, and to reduction in likelihood of catastrophic failure when weather is cold and where there are bad railway lines. The carbide-free bainite steel wheel has excellent strength and toughness and good resistance to thermal damage and rolling contact fatigue.

5. Conclusions

(1) The new experimental low-medium carbon Si-Mn-Mo-V steel, whose alloy design is reasonable and satisfies the design requirements of carbide-free bainite wheel steel, can be applied in wheel manufacture by suitable chemical composition and correct heat treatment for big wheels whose shapes are intricate. The microstructure of the rim is mainly carbide-free bainite, and those of the web and hub are both granular bainite and bainitic ferrite.

(2) The values of strength, hardness and plasticity of the carbide-free bainite wheel are high, and the yield strength and Charpy impact energy are much higher than those of pearlite-ferrite wheel steel especially. The force-displacement curves and fractographies reveal the excellent ability of resistance to crack initiation and propagation.

(3) The wheels manufactured with carbide-free bainite steel may provide improved performances, and eliminate or minimize the sensitivity to high transient thermal damage and prevent wheel breakage. Carbide-free bainite steels are emerging as a potential wheel material to replace conventional carbon grade steels to achieve a longer life even if for high speed and heavy axle-load coach and wagon transportation.

References

[1] Y.M. Zhou, Wheels an axles of Chinese railway locomotive and car meeting challenges of 21st century, [in] *Proceedings 12th International Wheelset Congress*, China Railway Society, Qingdao, 1998, p.10.

[2] D.T. Tan, Present condition and future development of axles and wheels of Chinese railways, [in] *Proceedings 12th Interntional Wheelset Congress*, China Railway Society, Qingdao, 1998, p.14.

[3] U.P. Singh, A.M. Popli, D.K. Jain, B. Roy, and S. Jha, Influence of microalloying on mechanical and metallurgical properties of wear resistant coach and wagon wheel steel, *J. Mater. Eng. Perform.,* 12(2003), No.5, p.573.

[4] J. Sun, K.J. Sawley, and D.H. Stone, Progress in the reduction of wheel spalling, [in] *Proceedings 12th International Wheelset Congress*, China Railway Society, Qingdao, 1998, p.18.

[5] P.J. Mutton and R. Boelen, Wheel developments for high axle load operations, [in] *Proceedings 4th International Heavy Haul Railway Conference*, IEAust, Brisbane, 1989, p.414.

[6] Z.X. Liu and H.C. Gu, Failure modes and materials performance of railway wheels, *J. Mater. Eng. Perform.*, 9(2000), No.5, p.580.

[7] B. Catot and F. Demilly, Contribution to improved steel grades for wheels for heavy freight traffic, [in] *Proceedings 10th International Wheelset Congress*, Sydney, 1992, p.229.

[8] D. Rai, D.K. Jain, R. Singh, and V. Godura, C-Mn-Nb-V steel for heavy duty locomotive wheel applications, [in] *Proceedings 10th International Wheelset Congress*, Sydney, 1992, p.213.

[9] T. Constable, R.Boelen, and E.V. Pereloma, The quest for improved wheel steels enters the martensitic phase, [in] *Proceedings 14th International Wheelset Congress*, Orlando, 2004, p.1.

[10] K.J. Sawley and J. Kristan, Development of bainitic rail steels with potential resistance to rolling contact fatigue, *Fatigue Fract. Eng. Mater. Struct.*, 26(2003), No.10, p.1019.

[11] H.K.D.H. Bhadeshia and D.V. Edmonds, The mechanism of bainite formation in steels, *Acta Metall.,* 28(1980), No.9, p.1265.

[12] F.B. Yang, B.Z. Bai, D.Y. Liu, K.D. Chang, D.Y. Wei, and H.S. Fang, Microstructure and properties of a carbide-free bainite/martensite ultra-high strength steel, *Acta Metall. Sin.* (in Chinese), 40(2004), No.3, p.296.

[13] A. Zarei Hanzaki, P.D. Hodgson, and S. Yue, Retained austenite characteristics in thermomechanically processed Si-Mn transformation-induced plasticity steels, *Metall. Mater. Trans. A,* 28A(1997), No.11, p.2405.

[14] H.S. Fang, Z.G. Yang, J.B. Yang, and B.Z. Bai, Research on bainite transformation in steels, *Acta Metall. Sin.* (in Chinese), 41(2005), No.5, p.449.

[15] T. Kazuyuki and U. Yasuo, Double-crystal spectrometer for laboratory EXAFS spectroscopy, *J. Rev. Sci. Instrum.,* 59(1988), No.7, p.1120.

[16] A.T. Shuvaev, B.Y. Helmer, T.A. Lyubeznova, *et al.*,

Laboratory diffractometer-based XAFS spectrometer, *J. Synchrotron Radiat.*, 1999, p.6.

[17] G.I. Rees and H.K.D.H. Bhadeshia, Bainite transformation kinetics. Part 1. modified model, *Mater. Sci. Technol.,* 8(1992), No.11, p.985.

[18] A. Airod and R. Petrov, Analysis of the trip effect by means of axisymmetric compressive tests on a Si-Mn bearing steel, *ISIJ Int.,* 44(2004), No.1, p.179.

[19] S.S. Babu, E.D. Specht, S.A. David, E. Karapetrova, P. Zschack, M. Peet, and H.K.D.H. Bhadeshia, In-situ observation of lattice parameter fluctuations in austenite and transformation to bainite, *Metall. Mater. Trans. A,* 36A(2005), No.12, p.3281.

[20] A.M. Streicher-clarke, J.G. Speer, D.K. Matlock, and B.C. de Cooman, Analysis of lattice parameter changes following deformation of a 0.19C-1.63Si-1.59Mn transformation induced plasticity sheet steel, *Metall. Mater. Trans. A,* 36A(2005), No.4, p.907.